Singer, R. M., & Fishman, W. H. (1975) in *Isozymes* (Markert, C. L., Ed.) pp 753-774, Academic Press, New York.
Speeg, K. V., Jr., & Harrison, R. W. (1979) *Endocrinology (Baltimore) 104*, 1364-1368.
Speeg, K. V., Jr., Azizkham, J. C., & Stromberg, K. (1976) *Cancer Res. 36*, 4570-4576.
Stigbrand, T. S., Millan, J. L., & Fishman, W. H. (1982) *Isozymes: Curr. Top. Biol. Med. Res. 6*, 93-117.
Struck, D. K., & Lennarz, W. J. (1977) *J. Biol. Chem. 256*, 1404-1411.
Sussman, H. H., Small, P. A., Jr., & Cotlove, E. (1968) *J. Biol. Chem. 243*, 160-166.
Tokumitsu, S. I. (1984) in *Human Alkaline Phosphatases: Progress in Clinical and Biological Research* (Stigbrand, T., & Fishman, W. H., Eds.) pp 185-205, Alan R. Liss, Inc., New York.
Wahl, G. M., Stern, M., & Stark, G. R. (1979) *Proc. Natl. Acad. Sci. U.S.A. 76*, 3683-3687.
Yanisch-Perron, C., Vieira, J., & Messing, J. (1985) *Gene 33*, 103-109.
Young, R. A., & Davis, R. W. (1983a) *Proc. Natl. Acad. Sci. U.S.A. 80*, 1194-1198.
Young, R. A., & Davis, R. W. (1983b) *Science (Washington, D.C.) 222*, 778-782.

Oligomerization and Ring Closure of Immunoglobulin E Class Antibodies by Divalent Haptens†

R. Schweitzer-Stenner,‡,§ A. Licht,‡ I. Lüscher,∥,⊥ and I. Pecht*,‡
Departments of Chemical Immunology and Membrane Research, The Weizmann Institute of Science, Rehovot 76100, Israel
Received September 4, 1986; Revised Manuscript Received February 5, 1987

ABSTRACT: Cross-linking of antibodies constitutes a widespread initiation signal for their respective effector functions. Cross-linking IgE-class antibodies provide the triggering signal to mast cells for their degranulation process. To obtain a quantitative insight into these cross-linking processes, the interactions between a DNP-specific monoclonal antibody of the IgE class and a series of divalent DNP haptens with spacers of different length and flexibility have been studied by fluorescence titration experiments. These were analyzed by employing the theoretical model developed by Dembo and Goldstein [Dembo, M., & Goldstein, B. (1978) *J. Immunol. 121*, 345-353] in a fitting procedure. Equilibrium constants that describe the aggregation and ring-closure processes caused by divalent hapten binding have been used as free parameters. The intrinsic binding constants were determined by fluorescence titrations with corresponding monovalent haptens. The main results are the following: (1) The divalent haptens with a short and flexible spacer [i.e., N^{α},N^{ϵ}-di-(DNP)-L-lysine, *meso*-bis[(DNP-β-Ala)amino]succinate, and bis[(DNP-tri-D-Ala)amino]heptane, having a maximal DNP–DNP distance of Γ = 14, 21, and 45 Å, respectively] effect aggregation of the antibodies mainly into closed dimers. (2) The divalent hapten family with long and rigid oligoproline spacers di-(DNP)-Ahx-Asp-$(Pro)_n$-Lys with n = 24, 27, and 33 (i.e., Γ = 100, 110, and 130 Å) causes aggregation of the antibodies predominantly into closed dimers and trimers. The corresponding equilibrium constants of the respective ring-closure processes decrease significantly with longer spacer length. (3) Evidence was found that intramolecularly monomeric ring closure of the IgE antibodies is caused by haptens containing oligoproline spacers with n = 37 or 42 (Γ = 130–150 Å). The equilibrium constant of the ring-closure process increases with spacer length. This increase in stability indicates a difference in the imposed strain. Furthermore, the latter results imply that the distance between the two binding sites of the IgE molecule lies in the range dictated by the rigid oligoproline part of the respective hapten's spacer, i.e., 115–130 Å. (4) Nearly all oligomeric ring-closure processes proceed relatively slowly with an approximate lower limit of a half-life of 5–10 s. This slowing down of the aggregation and ring-closure processes most probably reflects steric factors.

Antibodies of the IgE[1] class are responsible for the immunological pathway leading to degranulation of mast cells and basophils, thus initiating reactions of the immediate type of hypersensitivity. The first step of this process involves antigen-induced aggregation of cell-bound IgE antibodies (Ishizaka & Ishizaka, 1969; Segal et al., 1977; Kulczycki et al., 1974; Schlessinger et al., 1976; Menon et al., 1985, 1986a,b). One of the earliest ensuing events which this aggregation effects is the opening of Ca^{2+} channels, raising transiently the cytosolic free Ca^{2+} concentration (Foreman et al., 1977; Mazurek et al., 1983; Corcia et al., 1986). Further steps in this biochemical cascade lead to the eventual degranulation and release of the stored, preformed mediators such as histamine and serotonin and synthesis of new mediators, derivatives of arachidonic acid (Schwartz & Austen, 1984).

† This work was supported in part by the National Institutes of Health, NIAID Grant 5R01 A122669, and by the Council for Tobacco Research, USA, Inc., Grant 1818. R.S.-S. is a recipient of a Minerva fellowship (1985–1986).
* Author to whom correspondence should be addressed.
‡ Department of Chemical Immunology.
§ Permanent address: Fachbereich 1-Physik, Universität Bremen, 33 Bremen, FRG.
∥ Department of Membrane Research.
⊥ Present address: Department of Pathology, Washington University School of Medicine, St. Louis, MO 63110.

[1] Abbreviations: DNP, 2,4-dinitrophenyl; IgE, immunoglobulin E; IgG, immunoglobulin G; Lys, L-lysine; Gly, glycine; Ahx, 6-aminohexanoate; But, γ-aminobutyric acid; Asp, L-aspartate; $(Pro)_n$, polypeptide containing n L-proline(s); RMS, root mean square.

0006-2960/87/0426-3602$01.50/0

Table I: Interaction Parameters between Divalent DNP Haptens and IgE-A2 Antibodies Derived from the Fitting Procedure

(A) Monovalent Haptens

hapten	K_{int} (M^{-1})	q_1	hapten	K_{int} (M^{-1})	q_1
DNP-Gly	6.6×10^4	0.42	DNP-Ahx	3.5×10^6	0.36
DNP-Bu	1.2×10^6	0.38	DNP-Ahx-Asp-$(Pro)_{21}$	1.4×10^7	0.36

(B) Divalent Haptens

hapten	Γ (Å)	K_{int} (M^{-1})	K_{agg} (M^{-1})	J_1	J_2	q_1	$q_2 = q_3$
N^{α},N^{ϵ}-di(DNP)-Lys	14	4.3×10^5	2.6×10^4		139	0.45	0.53
meso-bis[(DNP-β-Ala)amino]succinate	21	1.1×10^6	9.2×10^4		60	0.42	0.28
bis[(DNP-tri-D-Ala)amino]heptane	45	3.3×10^6	3.4×10^5		26	0.44	0.70
di(DNP)-Ahx-Asp-$(Pro)_n$-Lys							
$n = 24$	105	1.0×10^7	7.2×10^6		82	0.33	0.37
$n = 27$	113	8.8×10^6	6.6×10^6		62	0.32	0.32
$n = 33$	132	1.0×10^7	5.2×10^6		7.0	0.32	0.42
$n = 37$	145	1.0×10^7	4×10^6	3.6		0.42	0.42
$n = 42$	160	1.0×10^7	4×10^6	9.6		0.38	0.38

Earlier studies of antibody–antigen reactions were not amenable to a satisfactory quantitative analysis because only polyclonal antibodies were available and characteristics of the antigens (e.g., number and spatial distribution of epitopes) were also heterogeneous and ill-defined. One-step in the effort to overcome these difficulties was made by employing divalent haptens with flexible spacers of different lengths to trigger the degranulation (Siraganian et al., 1975; Dembo et al., 1978, 1979a,b). Polyclonal antibodies, however, were still used in these experiments.

The respective divalent hapten–antibody interactions have been described in terms of a theory containing the analysis of the following aspects: (1) binding of IgE to Fc_ϵ receptors (Goldstein et al., 1979); (2) cross-linking of the cell-bound IgE antibody by divalent haptens (Dembo & Goldstein, 1978a); (3) mediators release as a function of the mole fraction of antibodies incorporated in a polymer (Dembo et al., 1977; Goldstein et al., 1979; DeLisi & Siraganian, 1979a,b); and (4) activation and desensitization of the cells (Goldstein et al., 1979).

These theoretical treatments yielded information concerning both the equilibrium constants of the hapten binding and the cross-linking process as well as estimates of the rates of histamine release and desensitization. More recently, the relationship between the size of the IgE oligomers and the extent of mediators release has been further investigated (Maeyama et al., 1986; Menon et al., 1986a,b). Both purified, preformed covalent oligomers of IgE as well as noncovalent cross-linking agents (like monoclonal anti-IgE antibodies) were employed. The results showed marked differences in response depending on the type of mast cells or basophils employed. Furthermore, difficulties in interpreting earlier results employing covalent oligomers were raised by the observation of large-scale clustering of the cell-membrane-bound small oligomers (Menon et al., 1984). All these findings suggested the need for a quantitative analysis of the IgE oligomerization processes.

The initiating step of the biochemical cascade is the binding and later on cross-linking of the IgE-class antibodies by their respective antigens. In this study, monoclonal DNP-specific IgE antibodies with a convenient affinity and chemically defined cross-linking agents were employed. The fluorescence titrations were carried out in homogeneous aqueous solution by using divalent haptens with spacers of different flexibility and length. The size of these haptens is described in terms of maximal hapten length Γ (Archer & Krakauer, 1977) defined by the equation

$$\Gamma = (5/3)^{1/2}\langle r_{DNP}^2\rangle^{1/2} \quad (1)$$

$\langle r_{DNP}^2\rangle^{1/2}$ is the root mean square value (RMS) of the distance between the centers of mass of the DNP groups. The following haptens were employed:

Group 1 consists of haptens with short and flexible spacers such as N^{α},N^{ϵ}-di(DNP)-Lys, *meso*-bis[(DNP-β-Ala)amino]-succinate, and 1,7-bis[(N^{α}-DNP-tri-D-Ala)amino]heptane with maximal lengths between 14 and 45 Å.

Group 2 consists of haptens with long and rigid spacers such as di(DNP)-Ahx-Asp-$(Pro)_n$-Lys (n = 24, 27, 33, 37, 42) with maximal lengths of 100, 110, 130, 140, and 155 Å, respectively.

Analysis of the different fluorescence titrations (Table I lists the employed divalent haptens and their respective maximal length) was performed by using the theoretical model developed by Dembo and Goldstein (1987a). This theory takes into account hapten binding to the antigen binding sites of the IgE, aggregation into oligomers, ring-closure processes in the different oligomeric states, and intramolecular bridging of the IgE–Fab arms.

In order to obtain the intrinsic binding constants of the different divalent haptens to the IgE-A2, we have performed fluorescence titrations of the respective monovalent haptens, i.e., DNP-Gly, DNP-But, DNP-Ahx, and DNP-Ahx-Asp-$(Pro)_{21}$. The equilibrium constants for aggregation and ring-closure processes induced by divalent hapten binding were obtained by fitting the experimentally obtained fluorescence titrations to a mathematical formalism derived from the Dembo–Goldstein theory (1978a). The stoichiometries and equilibrium constants obtained for the different antibody–hapten reactions provide some fundamental and interesting insights into the IgE-cross-linking and ring-closure processes occurring in homogeneous aqueous solution.

Materials and Methods

Preparation of the DNP-Specific IgE-A2 Antibodies. The hybridoma cell line secreting the DNP-specific monoclonal IgE-A2 was obtained from the ATCC (Rudolph et al., 1981). The cells were grown first in tissue culture and later injected intraperitoneally into mice (Balb/c × C57Bl/6)F_1 for propagation in the ascites. The IgE antibodies (line A2) were isolated by absorbing the ascitic fluid on a DNP-Lys–Sepharose 4B immunoadsorbant column. The antibodies were eluted with 2 column volumes of 0.1 M dinitrophenol solution in borate-buffered saline (0.2 M sodium borate pH 7.4, [NaCl] = 150 mM) and dialyzed extensively against the same buffer. Residual dinitrophenol was removed by passage through a Dowex 1.8, 100–200 mesh column (0.6 × 4 cm) in a solution consisting of 0.1 M NaCl and 0.01 M sodium phosphate buffer adjusted at pH 5.7. Finally, the antibodies were dialyzed extensively against 0.15 M NaCl, 0.2 M sodium borate buffer of pH 7.4.

Preparation of the Ligands. The monovalent DNP-glycine, DNP-But, and DNP-6-aminohexanoate and the divalent N^{α},N^{ϵ}-di(DNP)-L-lysine haptens were obtained commercially from Sigma and used without further purification.

meso-Bis[(N^{β}-DNP-Ala)amino]succinate was a kind gift from Dr. Verne Schumaker, UCLA. Bis[(N^{α}-DNP-tri-D-Ala)amino]heptane was synthesized as follows: First, the benzyloxycarbonyl-tri-D-Ala peptide was synthesized stepwise by the mixed anhydride method (Schechter & Berger, 1966). Then, 2 equiv of these tripeptides were conjugated to 1 mol of 1,7-diaminoheptane by the hydroxy succinimide ester method (Anderson, 1964) and the benzyloxycarbonyl groups were removed. Finally, the resulting 1,7-bis[(tri-D-Ala)amino]-heptane species was reacted with 2.2 equiv of 1-fluoro-2,4-dinitrobenzene to yield a precipitate of the bis[(DNP-tri-D-Ala)amino]heptane product. The product was suspended in chloroform, filtered, and washed with 0.5 M hydrochloric acid and 0.5 M sodium bicarbonate to remove unreacted (tri-D-Ala)-1,7-diaminoheptane and any free dinitrophenol, respectively. Its purity as a single band was shown by thin-layer chromatography in ethanol–acetic acid–water (7:1:2).

Fluorescence Titrations. The binding of haptens to the IgE-A2 antibodies was monitored continuously by measuring the quenching of the intrinsic antibody fluorescence. This effect is caused by nonradiative energy transfer to the DNP-groups of the bound haptens (Green, 1964). The measurements were performed on an MPF-44 Perkin-Elmer spectrofluorometer. The excitation wavelength was 280.0 ± 0.1 nm, and the emission was monitored at its maximum, i.e., 330.0 ± 0.1 nm. The adjusted bandwidth varied between 6 and 4 nm. The temperature of the sample was kept constant at 37 °C. The protein solution was filled into a spectrofluorometer cuvette with internal dimensions of 7 mm × 7 mm × 30 mm. The titrant solution was delivered continuously to the titrated solution in the cuvette by a motor-driven syringe. The rate of titration could be varied by changing the speed of the driving motor and/or the volume of the syringe. The experimental data were collected and digitized by a microcomputer (1020 data points for each titration) and submitted to the central computer of the Weizmann Institute, where it was stored on a disk for the analysis. The experimental parameters, i.e., antibody concentration, hapten sites concentration of the titrant solution, and titrant solution addition rate, required a special respective adjustment for each of the employed haptens and will be discussed in the next section.

In order to prepare our data for the analysis, the following corrections were made.

(1) The antibody and hapten concentrations and the fluorescence intensity were corrected for dilution by the equations:

$$A_T = A_{T0}V_0/(V_0 + V^+) \quad (2)$$

$$Q_T = Q_{T0}V^+/(V_0 + V^+) \quad (3)$$

$$\tilde{I}(Q_T,A_T) = \tilde{I}_0(V_0 + V^+)/V_0 \quad (4)$$

where A_{T0} is the antibody concentration of the sample and Q_{T0} labels the concentration of the titrant solution. A_T and Q_T are the free antibody and hapten concentration after the volume V^+ of the titrant solution is added to the antibody solution of volume V_0. The measured intensity is denoted by $\tilde{I}_0(Q_{T0},A_{T0})$ and the corresponding corrected values by $\tilde{I}$.

(2) The measured fluorescence titration was also corrected for the absorption of the DNP molecules (inner filter effect). This was carried out by titrating an immunoglobulin with nonrelated specificity (e.g., HOPC-8 or MOPC-104E). The

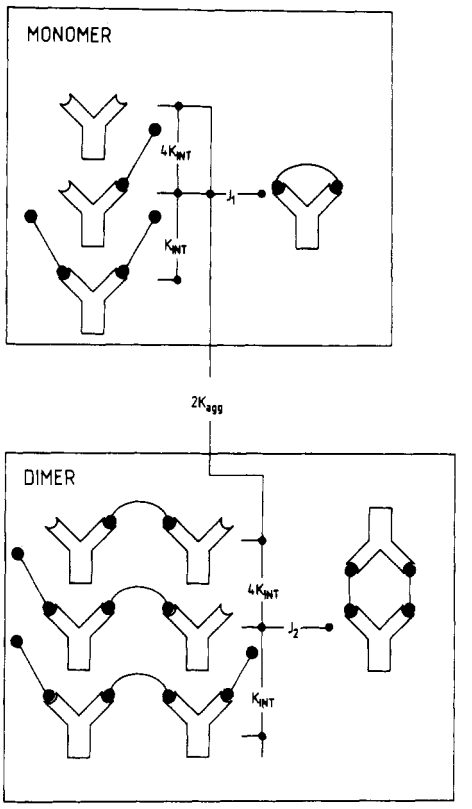

FIGURE 1: Scheme of the reactions between an IgE-class antibody and divalent haptens (●–●): K_{int}, intrinsic equilibrium constant of hapten binding to an antibody binding site; K_{agg}, equilibrium constant of the aggregation step; J_1 and J_2, equilibrium constant of the monomeric and dimeric ring-closure steps, respectively.

final expression for the fluorescence, denoted $I(Q_T,A_T)$, can be obtained by employing the equation

$$I(Q_T,A_T) = \frac{\tilde{I}(Q_T,A_T)I_{max}}{I_{ns}(Q_T,A_T)} \quad (5)$$

$I_{ns}(Q_T,A_T)$ labels the intensity of the nonspecific titration, and I_{max} is the initial fluorescence intensity due to the nonliganded antibody.

Theoretical Background

The basic equations of the theory used to analyze our data have been formulated by Dembo and Goldstein (1978a). These authors, however, developed this theory in order to calculate the maximal release of vasoactive amines from mast cells induced by divalent hapten binding to cell-bound IgE. Therefore, we find it necessary to outline its application to our experimental data (i.e., fluorescence titration of IgE antibodies with divalent haptens in homogenous solution).

Figure 1 illustrates the different processes caused by divalent hapten binding to IgE. These can be classified as follows:

(1) The first step of each reaction scheme is the binding of a divalent hapten H to its site on one Fab arm

$$\text{IgE} + \text{H} \underset{}{\overset{4K_{int}}{\rightleftharpoons}} (\text{IgE})(\text{H})$$

Employing a notation similar to that of Dembo and Goldstein, one can describe this reaction in terms of the mass-action law

$$4K_{int} = \frac{[1,1,0]}{[1,0,0]Q} \quad (6)$$

Q = [H] is the free hapten concentration. The concentration of the hapten–antibody complexes are denoted by $[i,j,m]$, which means that the complex contains i antibodies and j

haptens; m is equal to one if the complex is closed and to zero if it is open. The equilibrium constant K_{int} is defined by the intrinsic binding of a monovalent hapten to an Fab binding site. It is multiplied by a factor of 4, because both the hapten and the antibody are divalent. It should be noted that eq 6 is valid only in the absence of cooperativity.

(2) Three distinct pathways provide the second step.

(a) Binding of a second divalent hapten

$$(IgE)(H) + (H) \overset{K_{int}}{\rightleftharpoons} (IgE)(H)_2$$

This can be described by

$$K_{int} = \frac{[1,2,0]}{[1,1,0]Q} \tag{7}$$

(b) Binding of a free antibody to a hapten–IgE complex. The corresponding reaction scheme is given by

$$(IgE) + (IgE)(H) \overset{4K_{int}}{\rightleftharpoons} (IgE)_2(H)$$

The condition of equilibrium for this reaction producing open dimers is (cf. Figure 1)

$$K_{agg} = \frac{[2,1,0]}{[1,0,0][1,1,0]} \tag{8}$$

where K_{agg} is the corresponding equilibrium constant.

(c) Intramolecular ring closure of the liganded monomer, which is described by the equations

$$(IgE)(H) \overset{J_1}{\rightleftharpoons} ((IgE)(H))_{cyc}$$

$$J_1 = \frac{[1,1,1]}{[1,1,0]} \tag{9}$$

Note that J_1 is a dimensionless unimolecular equilibrium constant.

(3) In principle, these three independent pathways exist for all further aggregation states, i.e., formation of trimers, tetramers, etc. Aggregation is described by the interaction between an Fab binding site and the free end of a hapten–antibody complex. Therefore, the equilibrium between the different oligomerization steps is related by the same aggregation constant K_{agg}. This leads to the general equation for the nth oligomer.

$$(K_{agg})^{n-1} = \frac{[n,n-1,0]}{[1,1,0]^{n-1}[1,0,0]} \tag{10}$$

In this case, the free energy difference between subsequent oligomerization steps is always the same and, therefore, the occupation numbers of the different aggregation states decrease toward polymers of higher order. In other words, the dimer will be the most populated oligomeric state.

(4) A further, third, step exists for all polymeric states—the ring closure of a dimer, trimer, etc., which is described by the equations

$$(IgE)_n(H)_{n-1} + (H) \overset{4K_{int}}{\rightleftharpoons} (IgE)_n(H)_n$$

$$(IgE)_n(H)_n \overset{J_n}{\rightleftharpoons} ((IgE)_n(H)_n)_{cyc}$$

(5) The unimolecular equilibrium constant J_n of each oligomeric state can be calculated in terms of the dimeric constant J_2 to be

$$J_n = 4J_2/n^2 \qquad n \geq 2 \tag{11}$$

This is based on the following considerations (Archer & Krakauer, 1977):

There are $2n$ hapten–antibody bonds in a ring containing n antibody molecules. Since the rupture of each of these bonds occurs with equal probability, the rate constant for ring opening is proportional to n.

Ring closure can be interpreted in terms of a random walk process of n steps in two dimensions; therefore, the association is inversely proportional to n. Thus the equilibrium constant becomes inversely proportional to n^2 for $n \geq 2$.

Calculation of the Fluorescence Titration. Assuming that quenching by hapten of the antibody intrinsic emission is proportional to the number of occupied binding sites, one obtains for the observed fluorescence intensity

$$I(Q_T) = I_{max}[1 - qY(Q_T,K_{int},K_{agg},J_n)] \tag{12}$$

where Y denotes the mole fraction of the occupied sites. The calculation of Y is described in the Appendix. I_{max} is the initial fluorescence intensity obtained for $Q = 0$, and q is the respective quenching factor defined by

$$q = (I_{max} - I_{min})/I_{max} \tag{13}$$

I_{min} denotes the intensity of the quenched fluorescence.

If the length of the spacers of the employed haptens is in the same order of magnitude as the Förster radius (~40 Å), dipole–dipole interactions occur between bound DNP groups and the donors, tryptophan residues, of adjacent antibodies within the same oligomeric complex. Therefore, different quenching factors q have to be introduced, which are related to each distinct step of the hapten–antibody interactions, i.e., hapten binding ($j = 1$), oligomerization ($j = 2$), and ring closure ($j = 3$). This leads to a modified version of eq 12, which can be written as

$$I(Q_T) = I_{max}[1 - \sum_{j=1}^{3} q_j \chi_j(Q_T,K_{int},K_{agg},J_n)] \tag{14}$$

The function $\chi_j(Q_T,K_{int},K_{agg},J_n)$ represents the respective mole fraction of the occupied binding sites. Its calculation is described in the Appendix.

The equilibrium constants K_{agg}, J_1 and J_2 and the quenching factors q_1, q_2, and q_3 were used as free parameters in a fitting procedure. K_{int} has been derived from the titrations with the appropriate monovalent haptens. All fluorescent titrations performed with divalent haptens are fitted to eq 14. The fitting procedures were performed by using a modified Marquart algorithm as it has been described by Fletcher (1971).

It should be also mentioned that some of the divalent haptens employed in this study are slightly asymmetric (all the oligoproline ones), thus causing two different intrinsic binding constants, $K_{int,1}$ and $K_{int,2}$. Therefore the intrinsic binding constant differs for each of the attached DNP groups (cf. Table I). However, since the basic quantity for our calculation is $2K_{int}$, the two binding processes cannot be distinguished. Therefore, in this case, we use an intrinsic binding constant defined by $(K_{int,1} + K_{int,2})/2$ to characterize the hapten binding.

The equilibrium constants K_{agg}, J_1, and J_1 are slightly different for interactions with the distinct ends of the somewhat asymmetric haptens. Still, as one can learn from eq A14 and A15 of the Appendix, each of these constants is multiplied by the intrinsic constant K_{int}. This means that for asymmetric haptens the constants K_{agg}, J_1, and J_2 of side 2 are multiplied by the intrinsic constant of side 1 and vice versa. Since each of these constants depends linearly on their respective intrinsic constant (i.e., $K_{agg,1}$ depends on $K_{int,2}$, etc.), the products $K_{agg,j}K_{int,j'}$ ($j,j' = 1, 2; j \neq j'$) do not depend on the binding

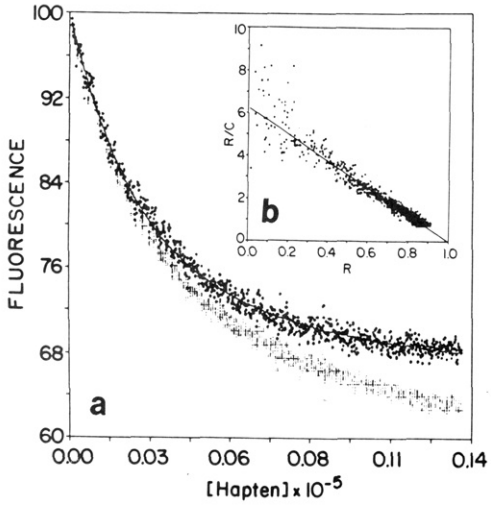

FIGURE 2: (a) Plot of the quenching of intrinsic antibody (IgE-A2) fluorescence as a function of the hapten (DNP-Ahx) concentration added (lower data set). The upper data set displays the fluorescence values corrected for the decrease in emission due to dilution and light absorption by the DNP groups (inner filter effect). The solid line drawn through these data points is the theoretical titration curve. (b, inset) Scatchard plot for the binding of the monovalent DNP-Ahx-hapten to IgE-A2 as calculated from the above titration.

site. Therefore, the use of slightly asymmetric divalent haptens does not limit the applicability of the theory outlined in this section.

Results and Discussion

In order to determine intrinsic binding constants of DNP haptens as effected by different side chains, fluorescence titrations with the following monovalent haptens were first performed: DNP-Gly, DNP-But, DNP-Ahx, and DNP-Ahx-Asp-$(Pro)_{21}$. These titrations were analyzed in terms of a single binding equilibrium process. For all monovalent haptens employed, this procedure yielded a satisfactory fit (the derived intrinsic binding constants are listed in Table I). The quality of the fit was checked by calculating the corresponding Scatchard plots as illustrated for the binding of DNP-Ahx (Figure 2b) to the IgE-A2 antibody.

It is interesting to note that the intrinsic binding constant increases significantly as the distance between the carboxylate group on the side chain and the center of the DNP ring increases. This probably reflects a subsite on the antibody to which an electrostatic interaction with the carboxylate group exists, providing an enthalpic contribution to the binding energy (Pecht et al., 1972). Whereas the performance and analysis of the titrations with monovalent haptens are relatively straightforward procedures, the application to divalent haptens requires a different choice of experimental parameters. This is due to the fact that several steps are involved in the binding process. The respective requirements of the parameters can be classified as follows:

(1) As can be learned from the Theoretical Background section, the aggregation into polymers at a given hapten concentration depends on the total antibody sites concentration. If the latter is too low, aggregation becomes negligible and cannot be detected in the fluorescence titration. This should be taken into account especially with the short divalent haptens. The aggregation equilibrium constants of these are expected to be nearly 2 orders of magnitude lower than the corresponding intrinsic constants (cf. Dembo & Goldstein, 1978b).

(2) If the intrinsic affinity is relatively high, as is the case for all oligoproline haptens, essentially all the added ligand may bind already at a rather low concentration. In this case, the system becomes undefined from the theoretical point of view. In order to avoid this, the antibody concentration should be lower than $(2K_{int})^{-1}$.

(3) The titrations with most of the divalent haptens employed in this study exhibit a significant dependence on the rate of hapten addition. This is probably due to the slow rates of the oligomerization and ring-closure processes (Dembo et al., 1978). In order to reach equilibrium conditions, one should choose rather slow hapten addition rates ($(2–5) \times 10^{-13}$ mol/s). Furthermore, in order to reach the required degree of saturation, an appropriate antibody concentration should be chosen.

(4) The concentration of the IgE-A2 antibody required in order to achieve a good signal-to-noise ratio and an accurate determination of the concentration should be higher than 3×10^{-8} M.

It is obvious that all these conditions impose a considerable restriction on the choice of the experimental parameters. In order to comply with these constraints, the following protocol was adopted:

(1) Assuming the simple geometric model proposed by Dembo and Goldstein (1978b), we calculated the expectation values for the equilibrium constant K_{agg}. These values were multiplied by a theoretical expectation value of 40 for the ring-closure equilibrium constant J_2 (Crothers & Metzger, 1972). This yields an estimate for the maximal affinity of the dimerization process. The inverse value of this product was used as a conservative lower limit for choosing the antibody concentration for the titrations.

(2) The titrations of all haptens employed were repeated at several different hapten addition rates (10^{-12}–10^{-13} mol/s). Each of the titrations was first analyzed in terms of a single binding constant and a stoichiometric factor. From this rough analysis, an effective affinity of the binding process could be derived. If two successive titrations performed at different addition rates yielded nearly the same effective affinity, the higher rate was adjusted for a further final titration. The procedure was considered to be completed if the effective affinity of the preceding measurements reproduced.

(3) For the short N^{α},N^{ϵ}-di(DNP)-Lys and *meso*-bis-[(DNP-β-Ala)amino]succinate this procedure could not be carried out completely since exceptionally low addition rates of the titrant were required. Therefore titrations usually took at least 3 h. Even then we could not ascertain that equilibrium was achieved since the titrations were not extended to longer periods because of inherent experimental instabilities. Despite this shortcoming, reasonable fits of the respective titrations could be achieved.

The different fluorescence titrations performed (experimental parameters are listed in Table II) were analyzed by the following steps:

(1) First, the fit of the data to a model describing a binding process that does not involve oligomerization or intramolecular ring closure is examined. No satisfactory fit could be achieved for this model to any of the titrations performed.

(2) The second step of analysis included the aggregation or the monomeric intramolecular ring closure (corresponding parameters K_{agg} and J_1). For analyzing these processes we used the intrinsic binding constants of the respective monovalent haptens as initial values in order to adjust these parameters to the right order of magnitude (i.e., DNP-But and DNP-Gly for N^{α},N^{ϵ}-di(DNP)-Lys, DNP-But for *meso*-bis-[(DNP-β-Ala)amino]succinate, DNP-Ahx for bis[(DNP-tri-D-Ala)amino]heptane, DNP-Ahx-Asp-$(Pro)_{21}$ and DNP-Ahx for di(DNP)-Ahx-Asp-$(Pro)_n$-Lys (n = 24, 27, 33, 37,

Table II: List of Experimental Conditions Used in Designing Titrations with Divalent Haptens

hapten	[IgE] (M)	[hapten] (M)	time used for one titration (s)	rate of hapten addition (mol/s)
N^{α},N^{ϵ}-di(DNP)-Lys	5.8×10^{-7}	2.0×10^{-4}	10800	2.7×10^{-13}
meso-bis[(DNP-β-Ala)amino]succinate	1.1×10^{-7}	2.0×10^{-5}	9000	2.8×10^{-13}
bis[(DNP-tri-D-Ala)amino]heptane	5.7×10^{-8}	7.5×10^{-6}	7200	1.1×10^{-13}
di(DNP)-Ahx-Asp-$(Pro)_n$-Lys				
$n = 24$	5.7×10^{-8}	6.3×10^{-6}	1800	1.4×10^{-13}
$n = 27$	5.7×10^{-8}	6.3×10^{-6}	1800	1.4×10^{-13}
$n = 33$	5.7×10^{-8}	6.3×10^{-6}	1800	1.4×10^{-13}
$n = 37$	5.7×10^{-8}	6.3×10^{-6}	1800	1.4×10^{-13}
$n = 42$	5.7×10^{-8}	1.5×10^{-6}	720	1.1×10^{-13}

42)). The guess values for K_{agg} were calculated by applying the geometric model of Dembo and Goldstein (1978a).

(3) If step 2 did not yield a satisfactory fit, the equilibrium constant J_2 of the polymeric ring-closure step was introduced as an additional free parameter. In order to obtain further improvement of the fit, we examined varying extents of the respective fluorescence quenching by the different aggregation states.

This strategy of employing the fitting procedure enabled us to discriminate between distinct steps of antibody–hapten interaction because of the different respective stoichiometries involved (i.e., hapten to antibody 2:1 for a fully occupied monomer, $(n + 1)/n$ for a liganded polymer of nth order, and 1:1 for all closed states). Nevertheless, one should take into account that correlations between the different parameters can yield nonunique results. In order to avoid this fundamental difficulty, the following procedure has been carried out. In a first cycle, the equilibrium constants K_{int} and K_{agg} were used as fixed parameters. From the remaining free parameters, the unimolecular constants J_1 and J_2 exhibit some correlation with the quenching constant q_3, which reflects the more pronounced fluorescence quenching of the closed rings (cf. eq 14). This correlation, however, is restricted to a small interval which could be fixed by the fitting procedure. In a final run, K_{int} and K_{agg} were varied to improve the quality of the fits.

One further comment is due concerning the principles of our analysis: We have tried to fit the fluorescence titration data assuming that a higher oligomeric state is favored because of its enthalpic advantage (Schumaker et al., 1973). In order to derive the formalism describing this process, different constants for the ring-closure processes in higher order oligomers that cannot be described in terms of J_2 should be considered. However, all calculations based on the assumption that higher order oligomers significantly contribute to the fluorescence titration led to rather poor fits and unreasonable values for the J_n parameter. Therefore, we concluded that even though the validity of eq 11 cannot be proved, the applied model is a suitable tool for analyzing the investigated hapten–antibody interactions.

As a result of this fitting procedure, satisfactory agreement between the calculated and experimental titration curves has been usually obtained. The statistical error in the measured emission intensity lies between 2 and 3%. The corresponding uncertainty in the fitting parameter is significantly lower than the errors caused by the correlations between the fitting parameters (~10–15%). The resulting parameters, i.e., the equilibrium constants of the different binding steps and their fluorescence quenching values, are presented in Table I. These can be classified as follows:

(1) *The short and flexible haptens* (maximal hapten length of 14–50 Å) cause some aggregation, mainly into a closed dimer. Higher oligomers appear in relatively low concentrations (<1%) and can therefore be neglected. The maximal amount of antibodies in the dimeric state varies between 15%

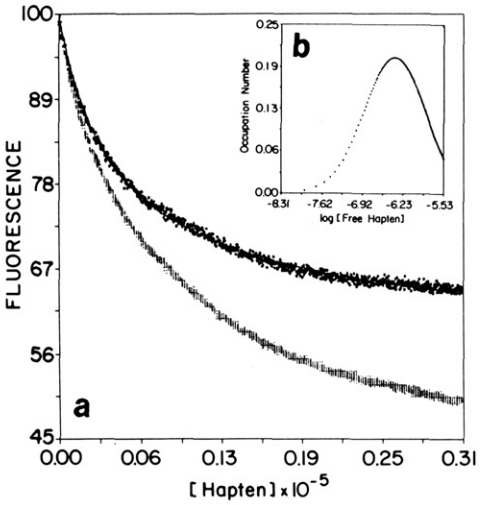

FIGURE 3: (a) Fluorescence quenching titration of the IgE-A2 by the divalent hapten *meso*-bis[(DNP-β-Ala)amino]succinate. The upper data points are corrected for the reduction in emission due to dilution and the inner filter effect. The extended line is the theoretical titration curve. (b, inset) Plot of the mole fraction of antibody molecules incorporated into dimers upon reaction with *meso*-bis[(DNP-β-Ala)amino]succinate vs. the logarithmic value of the free hapten concentration. More than 95% of the dimers are closed.

Table III: Distributions of Maximal Mole Fraction of Antibodies Incorporated in Dimers, Trimers, and Tetramers for the Respective Hapten–Antibody Complexes

	dimers (%)	trimers (%)	tetramers (%)
N^{α},N^{ϵ}-di(DNP)-Lys	35	0.4	6×10^{-3}
meso-bis[(DNP-β-Ala)amino]succinate	20	0.3	4×10^{-3}
bis[(DNP-tri-D-Ala)amino]heptane	17	0.1	7×10^{-3}
di(DNP)-Ahx-Asp-$(Pro)_n$-Lys			
$n = 24$	86	0.6	4×10^{-2}
$n = 27$	70	2.3	0.1
$n = 33$	35	5	1×10^{-2}
$n = 37$	4	0.3	1×10^{-2}
$n = 42$	1	0.3	1×10^{-2}

and 40%. The fraction of the higher oligomers is negligible because of the low values of the equilibrium constants for oligomerization. The calculated equilibrium constant for the dimeric ring-closure process decreases with larger spacer lengths. This type of divalent hapten binding is illustrated in Figure 3, which shows the fluorescence titration with *meso*-bis[(DNP-β-Ala)amino]succinate and a plot of the respective mole fraction of antibodies in the dimeric state vs. the free hapten concentration. The latter exhibit a maximum at a free hapten concentration of $Q_{max} = (2K_{int})^{-1}$. The calculated values of maximal mole fraction of antibodies in dimers are listed in Table III.

(2) *For long and rigid haptens*, Figure 4 shows titrations performed with the divalent haptens containing oligoproline spacers with $n = 24$ (a), $n = 27$ (b), and $n = 33$ (c). Derived

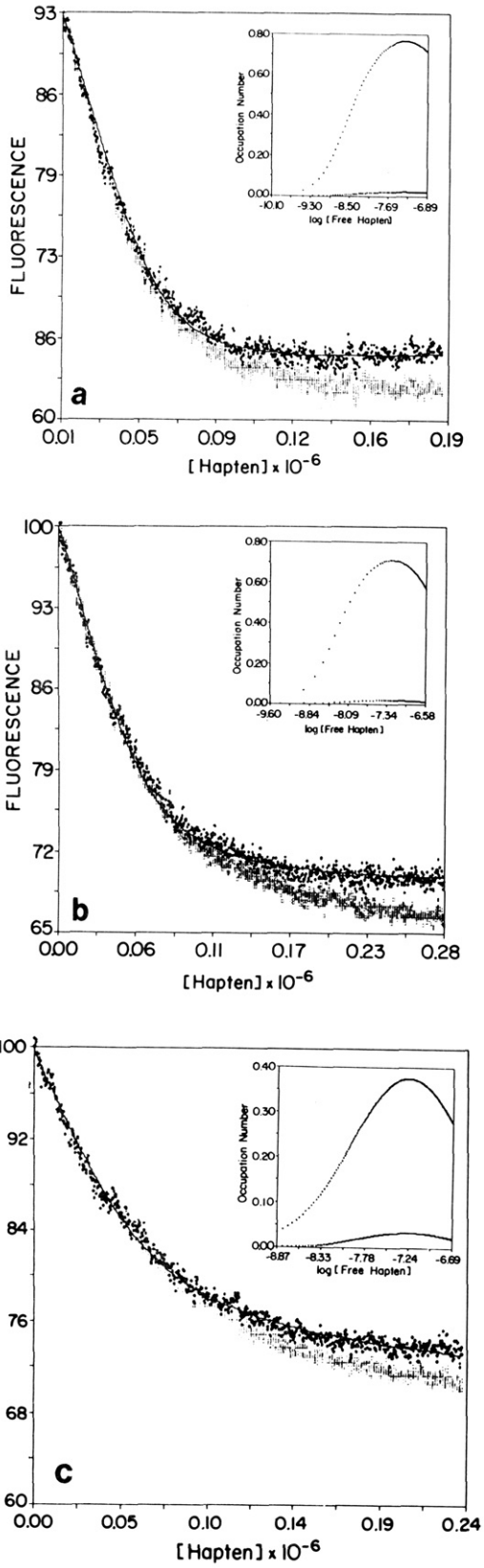

FIGURE 4: (a–c) Fluorescence titration of IgE-A2 by di(DNP)-Ahx-Asp-(Pro)$_n$-Lys (n = 24 (a), 27 (b), 33 (c)) (lower data sets). The upper sets display the corrected fluorescence due to dilution and inner filter effect. Solid lines drawn are the calculated best-fit curves. Insets: Plots of the mole fraction of IgE-A2 molecules incorporated in dimers (upper curve) and trimers (lower curve) upon reaction with the respective divalent haptens as a function of the logarithmic value of their free concentration. (All concentrations expressed in moles of divalent molecules.) 99, 98, and 85% of these dimers are closed rings, respectively.

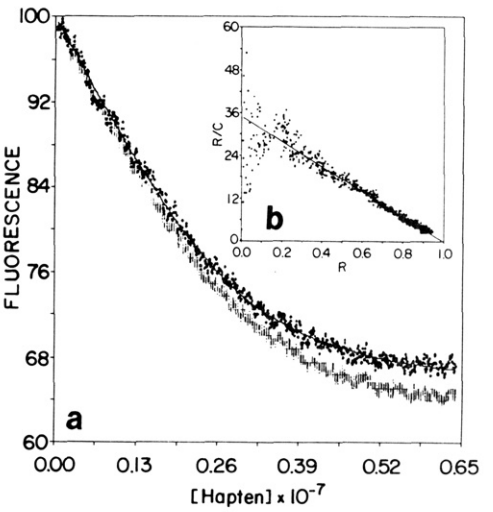

FIGURE 5: (a) Fluorescence titration of IgE-A2 by di(DNP)-Ahx-Asp-(Pro)$_{42}$-Lys (lower data set). The upper set displays the corrected fluorescence value due to dilution and inner filter effect. Solid line drawn is the calculated best-fit curve. (b, inset) Scatchard plot constructed from above titration.

from these titrations are the mole fractions of antibodies incorporated in dimers and trimers as a function of free hapten concentration (Figure 4 insets). One observes in these titrations that the effective affinity of haptens to antibody significantly decreases with longer spacers. This correlates with a decrease in dimerization (maximum mole fraction of antibodies in dimers 86% for n = 24, 75% for n = 27, and 30% for n = 33) and an increase of trimerization (1% for n = 24, 2% for n = 27, and 5% for n = 33). This is due to a slight decrease in K_{agg} (cf. Table II), which determines the ratio between the oligomeric states, and a respective significant decrease in the polymeric ring-closure J_2 (cf. Table II).

(3) The haptens with oligoproline spacers of length n = 37 and 42 exhibit a different behavior compared with their shorter homologues. Titrations with both haptens could be fitted by assuming only two steps of ligand–antibody interactions—hapten binding to the antibody and a subsequent intramolecular ring closure. In this case the binding process can be approximated by one equilibrium constant (cf. eq A4 of the Appendix). Therefore a Scatchard plot could be constructed from the titrations of both haptens. Figure 5 shows a titration with the n = 42 oligoproline hapten and the respective Scatchard plot. From the fitting procedure, one obtains the equilibrium constants J_1 = 3.6 and 9.6 for the haptens with n = 37 and 42, respectively.

The equilibrium constants K_{agg} *and* J_2 can be used to calculate the RMS values of the distances between the open ends, i.e., the unoccupied Fab sites of the respective dimers. This was carried out by employing the equation

$$\langle r^2\rangle_{dim}^{1/2} = \left(\frac{K_{agg}}{\rho J_2}\right)^{1/3} (3/2\pi)^{1/2} \qquad (15)$$

derived by Schumaker et al. (1980). The factor ρ = 0.6 nm^{-3} M^{-1} has to be inserted in order to take into consideration the particle density in the standard state (Archer & Krakauer, 1977). As illustrated in Figure 6, the distances between the unoccupied antigen binding sites show an essentially linear dependence on Γ, the calculated maximal length of the divalent haptens.

It is interesting to compare the $\langle r^2\rangle_{dim}^{1/2}$ values calculated by eq 15 with the results obtained from a geometric calculation of the polymer length. Assuming the internal rotation of the

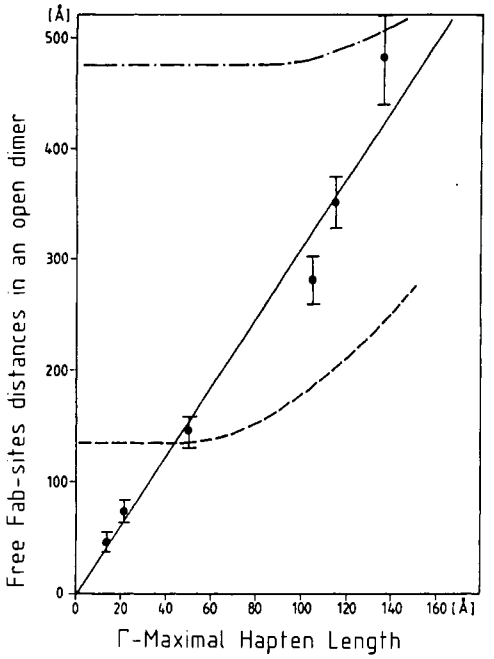

FIGURE 6: Plot of the end-to-end distance between the unoccupied antigen binding sites in an open IgE-A2 dimer vs. Γ, the maximal divalent hapten length. The extended line (—) displays the linear fit to the values (●) calculated by inserting the obtained J_2 values for the dimeric ring closure into eq 18. The dashed (– –) and dot-dashed (—·—) lines illustrated the end-to-end distance of a flexible and a maximally extended open dimer, respectively.

hapten–antibody complex to be unrestricted, we can calculate the end-to-end distance by

$$\langle r^2\rangle_f^{1/2} = (\sum_j l_j^2)^{1/2} \qquad (16)$$

where f denotes that the equation is valid for flexible polymers only and l_j is the length of the dimeric segments. These are defined as follows:

(1) For the complexes formed by short and flexible haptens, the segments of the complex, i.e., the Fab domains of the antibodies, are connected by flexible springlike elements of limited to negligible length, i.e., the immunoglobulin's hinge and switch regions and the short flexible haptens. Hence the dimer contains $j = 12$ segments (3 segments per Fab arm).

(2) For the dimeric complexes formed by long and rigid haptens, their intrinsic length cannot be neglected. However, since these haptens have flexible ends (≈15 Å per binding site), the rigid oligoproline part can be considered as further segments of the complex, whereas the flexible ends provide the connection to the adjacent Fab arms.

In order to employ this simple model, a length of 40 Å for the Fab domains of IgE molecules has been assumed from structural data reviewed by Poljak (1978). In Figure 6, the calculated end-to-end distances are presented by the lower dashed line. For small spacers (14–30 Å), $\langle r^2\rangle_f^{1/2}$ is significantly larger than $\langle r^2\rangle_{dim}^{1/2}$. For Γ = 40 Å, eq 15 and 16 yield nearly identical results, and for longer spacers $\langle r^2\rangle_f^{1/2}$ is smaller than $\langle r^2\rangle_{dim}^{1/2}$.

To provide a further reference, we calculated also the maximal length r_{max} of the polymer by using the equation

$$r_{max} = \sum_j l_j \qquad (17)$$

The segmental lengths were used as defined above. The upper dot-dashed line in Figure 6 represents the results of this calculation. For short spacers, r_{max} is an order of magnitude larger than the end-to-end distance $\langle r^2\rangle_{dim}^{1/2}$ calculated from our data, but at larger spacer lengths one obtains an asymptotic

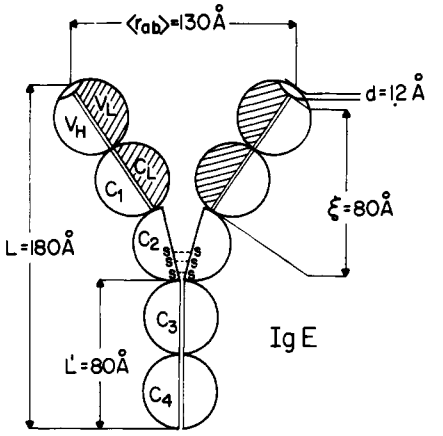

FIGURE 7: Schematic drawing of an IgE: V_H and V_L are the variable domains of the heavy and light chains, respectively; C_1, C_2, C_3, the different constant domains; –S–S, disulfide bonds in the hinge region. The concept of this drawing has been taken from Baird and Holowka (1985).

approach of $\langle r^2\rangle_{dim}^{1/2}$ to $\langle r^2\rangle_f^{1/2}$.

The three different plots shown in Figure 6 are tentatively explained by the following considerations: For short spacers (≈30 Å), the connection between adjacent Fab arms is short and probably less flexible because of steric hindrance. This is due to the fact that a large part of the haptens (≤12 Å) resides inside the binding sites. In this case the end-to-end distance is mainly determined by the flexibility of the Fab domains. Since the $\langle r\rangle_{dim}^{1/2}$ values calculated for the short haptens are significantly smaller than expected for a free flexible oligomer, they reflect a restriction of the segmental flexibility of the antibody.

This can be quantitatively expressed in terms of free energy ξ_{dim}, which probably reflects strain (Schumaker et al., 1973). In order to achieve this, the following equation has been applied:

$$\xi_{dim} = \frac{3}{2}RT[\ln \langle r^2\rangle_f - \ln \langle r^2\rangle_{dim}] \qquad (18)$$

Inserting the respective values for N^{α},N^{ϵ}-di(DNP)-Lys (Γ = 14 Å) yields 10.5 kJ/mol. For flexible haptens with longer spacers [≥30 Å, in the case of bis[(DNP-tri-D-Ala)amino]-heptane], the stretch of hapten residing within the binding site can be neglected. Hence, the intermolecular connections between Fab domains become more flexible. Therefore, one expects, in terms of our model, that the difference between $\langle r^2\rangle_{dim}^{1/2}$ and $\langle r^2\rangle_f^{1/2}$ should be much less than for the shorter haptens. This is indeed the case as one can see from Figure 6. The data obtained for the haptens with oligoproline spacers also fit our interpretation. As has been mentioned above, these haptens have two flexible ends with lengths that add up to nearly 30 Å. Since these ends can be regarded as flexible but of negligible length, one expects, in light of the above considerations, that the corresponding dimers and trimers are relatively more flexible than those containing shorter haptens. This is in accordance with the relatively small difference between $\langle r^2\rangle_f^{1/2}$ and $\langle r^2\rangle_{dim}^{1/2}$ obtained for long haptens.

We observed that only haptens with $n = 37$ and 42 oligoproline spacers cause intramolecular ring closure upon binding to the IgE-A2 antibody. The oligoproline parts are rigid with lengths of 115 and 130 Å, respectively. It is reasonable to assume that the rigid parts of the spacers dictate the minimal distance between the antigen binding site of the respective haptens. Therefore, one expects that the minimal distance between the antigen binding sites of the free IgE-A2 antibody is not significantly less than the length of the rigid parts of

the $n = 37$ hapten, i.e., 115 Å. Considering the dimensions proposed by Baird and Holowka (1985) for IgE molecules (cf. Figure 7), one calculates the corresponding angle ϕ_{min} between the Fab arms to be $\sim 60°$.

It is interesting to compare this result with the properties of polyclonal IgG-class antibodies. Schumaker et al. (1980) have analyzed the sedimentation patterns of complexes formed between IgG antibodies and small divalent haptens. From this they estimate the minimal angle between the Fab arms to be also close to 60°. Luedtke et al. (1981) have measured the resonance energy transfer between a fluorescent donor and an acceptor, both bound to Fab binding sites of the same chimeric IgG antibodies. From the experimental data, they calculate a mimimal angle of 40°–50°. Neither result differs considerably from those obtained in the present study. This indicates that in both classes of immunoglobulins a similar *average* angle is maintained between the two Fab arms.

It should be further noted that even the J_1 value, i.e., affinity for intramolecular ring closure derived from the titration with the $n = 42$ oligoproline hapten, is much lower than expected. This can be obtained from the application of the equation

$$J_{1,c} = \frac{K_{int}}{\rho\left[\frac{2\pi}{3}\langle r_{ab}^2\rangle\right]^{3/2}} \tag{19}$$

describing the relation between the equilibrium constant J_1 and the distance r_{ab} between the binding sites of the Fab arms. Assuming $\langle r_{ab}^2\rangle^{1/2}$ to be 140 Å (cf. the geometric model proposed by Baird and Holowka, which is illustrated in Figure 7), one calculates $J_{1,c}$ to be 1500. The large difference between this calculated value and that obtained from our data is most probably due to a strain energy induced by the intramolecular cross-linking process, which can be calculated by using the equation

$$\xi_{mon,2} = RT[\ln J_{1,c} - \ln J_1] \tag{20}$$

where $\xi_{mon,2}$ denotes the strain energy. Inserting the respective values yields $\xi_{mon,2} = 13$ kJ/mol.

It should be emphasized that the thus calculated strain is in the same order of magnitude as that deduced from the properties of the dimeric ring closure caused by the binding of short, flexible haptens.

Finally, we turn to the remaining equilibrium constants.

The intrinsic binding constant K_{int} used to fit the titrations differs only slightly from initial values obtained in the titrations with monovalent haptens.

The calculated aggregation constants are also in good agreement with the intrinsic values calculated by applying the simple geometric model developed by Dembo and Goldstein (1978b). This is an indication for both the validity of this model and the applicability of our fitting procedure.

Some final comments are due concerning the extensive fluorescence quenching caused by the distinct steps of hapten binding. The first step of the reaction, i.e., the binding of haptens to the Fab binding site, causes a fluorescence quenching of 35–45%. The respective quenching in the closed dimeric state is significantly higher for the binding processes of N^{α},N^{ϵ}-di(DNP)-Lys (53%) and bis[(DNP-tri-D-Ala)-amino]heptane (70%), but relatively low for *meso*-bis-[(DNP-β-Ala)amino]succinate (≈30%). At first sight, this is a surprising result. However, one should take into account that different processes influence the quenching in the closed oligomeric states.

(1) The binding of monovalent and divalent haptens to antibodies induces a significant spectral shift of the DNP absorption band toward longer wavelengths (Warner & Schumaker, 1970; Wilder et al., 1975). This shift is a factor of 4–5 times larger for divalent haptens (≈12 nm) than for monovalent ones (2–3 nm). This could be due to the aggregation process. Another reason for the shift in absorption bands of the bound haptens is most probably caused by their different side chains, e.g., an α-amine group in the bis-[(DNP-tri-D-Ala)amino]heptane vs. an ε-amine on lysine or a β-amine of alanine. Therefore one can deduce from these experimental findings that the spectral overlap with the IgE emission band decreases in some cases by the aggregation process, thus reducing fluorescence quenching.

(2) Since all short divalent haptens employed have a maximal length of less than 50 Å, dipole–dipole interaction between the DNP group and the donors of the adjacent antibody in the polymer is expected to contribute to the quenching process. This would cause an increased quenching in the oligomeric state of the hapten–antibody complex.

(3) This intermolecular quenching, however, is probably influenced by electric charges present on the spacers of the employed haptens. It is interesting to note in this context that the divalent hapten with two point charges on the spacer (*meso*-bis[(DNP-β-Ala)amino]succinate) induces relatively low quenching in the polymeric state, whereas the uncharged bis[(DNP-tri-D-Ala)amino]heptane causes a respective enhanced quenching. This may suggest a screening of the dipole–dipole interaction by the spacer charges, thus lowering fluorescence quenching.

The main results of this study can be summarized as follows:

(1) All divalent haptens employed, with the exception of the oligoproline haptens with $n = 37$ and 42, cause oligomerization into predominantly closed dimers. Additionally, the rigidly spaced divalent haptens effect the formation of some closed trimers.

(2) For both the short and the long haptens, the equilibrium constant of the polymeric ring closure decreases with increasing spacer length.

(3) The oligoproline haptens with $n = 37$ and 42 effect nearly exclusively an intramolecular ring closure.

A main aim of our work is to construct divalent hapten–antibody systems that can be well-defined in terms of their physicochemical properties. The application of such systems to the cellular level could provide a system where quantitative information is obtained about the relationship between the initial triggering process and the final release of vasoactive amines. Parallel experiments, therefore, would be performed by measuring Ca^{2+} influx and cell degranulation triggered by the divalent haptens employed in this study. Furthermore, it is important to analyze in detail the slow process of polymeric ring closure since this may provide information about the internal diffusion of respective open dimers. Finally, it would be interesting to obtain data by other physicochemical methods, e.g., electron microscopy, to corroborate the above conclusions.

APPENDIX

The reaction scheme presented in Figure 1 illustrates the principal states occupied by monomeric and dimeric species. There are four states for each oligomer of *n*th order. The respective concentrations can be calculated by the application of the mass–action law. This leads to the equations:

$$S_{n,0} = [n,n-1,0] = 4K_{int}K_{agg}QAS_{n-1,0} \tag{A1}$$

$$S_{n,1} = [n,n,0] = 4K_{int}QS_{n,0} \tag{A2}$$

$$S_{n,2} = [n+1,n,0] = 4K_{int}^2Q^2S_{n,0} \tag{A3}$$

$$S_{n,3} = [n,n,1] = 4K_{int}JQS_{n,0} \quad (A4)$$

$S_{n,0}$ labels the concentration of the open oligomer with two unoccupied binding sites. In the $S_{n,1}$ state, one of these sites is occupied by a hapten. $S_{n,2}$ denotes the concentration of the fully occupied oligomer, and $S_{n,3}$ denotes the concentration of the closed oligomer.

All relevant functions can now be calculated in terms of the quantities $S_{n,i}$ ($i = 0, 1, 2, 3$) as follows:

(a) free hapten (Q) and antibody (A) concentrations

$$A_T = \sum_{n=1}^{\infty}(n\sum_{i=0}^{3}S_{n,i}) \quad (A5)$$

$$Q_T = \sum_{n=1}^{\infty}(n\sum_{i=0}^{3}S_{n,i} - S_{n,0}) = A_T - \sum_{n=1}^{\infty}S_{n,0} \quad (A6)$$

(b) mole fraction of occupied binding sites

$$Y = \frac{A_T - \sum_{n=1}^{\infty}(S_{n,2} + S_{n,3} - S_{n,0})}{2A_T} \quad (A7)$$

(c) mole fraction of the occupied binding sites due to

(c1) hapten binding to an antibody free binding site

$$\chi_1 = \frac{\sum_{n=1}^{\infty}(S_{n,1} + 2S_{n,2})}{2A_T} \quad (A8)$$

(c2) aggregation into an open oligomer

$$\chi_2 = \frac{\sum_{n=1}^{\infty}(n-1)\sum_{i=0}^{2}S_{n,i}}{2A_T} \quad (A9)$$

(c3) oligomeric ring closure

$$\chi_3 = \frac{\sum_{n=1}^{\infty}2(n-1)S_{n,3}}{2A_T} \quad (A10)$$

(d) mole fraction of antibodies incorporated into an oligomer of the nth order

$$X_{A,n} = n\sum_{i=0}^{3}S_{n,i} \quad (A11)$$

In order to illustrate the procedure, explicit summation is carried out in eq A5 and A6. Insertion of eq A1–A4 yields

$$A_T = \sum_{n=0}^{\infty}n[(1 + 2K_{int}Q)^2 + 4K_{int}J_nQ]S_{n,0} \quad (A12)$$

$$Q_T = A_T - \sum_{n=0}^{\infty}S_{n,0} \quad (A13)$$

Each state $S_{n,0}$ can be expressed in terms of the free hapten and antibody concentrations by employing eq 6 and 10. This leads to

$$A_T = (1 + 2K_{int}Q)^2\sum_{n=0}^{\infty}n(4K_{int}K_{agg}Q)^{n-1}A^n + 4K_{int}Q\sum_{n=0}^{\infty}nJ_n(4K_{int}K_{agg}Q)^{n-1}A^n \quad (A14)$$

$$Q_T = A_T + Q - (1 - 4K_{int}^2Q^2)\sum_{n=0}^{\infty}(4K_{int}K_{agg}Q)^{n-1}A^n \quad (A15)$$

Applying the relations

$$\sum_{\beta=0}^{\infty}(\alpha + \beta\gamma)q^\beta = \frac{\alpha}{1-q} + \frac{\gamma q}{(1-q)^2} \quad (A16)$$

$$\sum_{\beta=1}^{\infty}\frac{q^\beta}{\beta} = \ln(1-q) \quad (A17)$$

$$(|q| < 1)$$

and using eq 11, one obtains

$$A_T = \frac{(1 + 2K_{int}Q)^2A}{(1 - 4K_{int}K_{agg}QA)^2} - \frac{2J_2\ln[1 - 4K_{int}K_{agg}QA]}{K_{agg}} + 4K_{int}QA[J_1 - 4J_2] \quad (A18)$$

$$Q_T = A_T + Q - \frac{(1 - 4K_{int}^2Q^2)A}{(1 - 4K_{int}K_{agg}QA)} \quad (A19)$$

In order to calculate the free hapten and antibody concentrations, we have solved eq A18 and A19 simultaneously by applying a two-dimensional version of the Newton–Raphson method (Margenau & Murphy, 1956) in a zero search program.

The other quantities introduced above can be derived in a similar way. Since they depend explicitly on Q and A, the solution of eq A18 and A19 is required for the calculation of the respective fluorescence titration curves.

REFERENCES

Anderson, G. W., Zimmermann, J. E., & Calletan, F. M. (1964) *J. Am. Chem. Soc. 86*, 1835–1841.

Archer, B. G., & Krakauer, H. (1977) *Biochemistry 16*, 618–627.

Baird, B., & Holowka, D. (1985) *Biochemistry 24*, 6252–6259.

Corcia, A., Schweitzer-Stenner, R., Pecht, I., & Rivnay, B. (1986) *EMBO J. 5*, 849–854.

Crothers, M. C., & Metzger, H. C. (1972) *Immunochemistry 9*, 341–357.

DeLisi, C., & Siraganian, P. (1979a) *J. Immunol. 122*, 2286–2292.

DeLisi, C., & Siraganian, P. (1979b) *J. Immunol. 122*, 2293–2299.

Dembo, M., & Goldstein, B. (1978a) *J. Immunol. 121*, 345–353.

Dembo, M., & Goldstein, B. (1978b) *Immunochemistry 15*, 307–313.

Dembo, M., Goldstein, B., Sobotka, A. K., & Lichtenstein, L. M. (1978) *J. Immunol. 121*, 354–358.

Dembo, M., Goldstein, B., Sobotka, A. K., & Lichtenstein, L. M. (1979a) *J. Immunol. 122*, 518–528.

Dembo, M., Goldstein, B., Sobotka, A. K., & Lichtenstein, L. M. (1979b) *J. Immunol. 123*, 1864–1872.

Fletcher, R. (1971) in *Harwell Subroutine Library*, Subroutine VB01A, Atomic Energy Research Establishment, Harwell, U.K.

Foreman, J. C., Hallett, M. B., & Mongar, I. L. (1977) *J. Physiol. 271*, 193–214.

Goldstein, B., Dembo, M., Sobotka, A. K., & Lichtenstein, L. M. (1979) *J. Immunol. 123*, 1873–1852.

Green, N. M. (1964) *Biochem. J. 90*, 564–568.

Ishizaka, K., & Ishizaka, T. (1969) *J. Immunol. 103*, 588–595.

Kulczycki, A., & Metzger, H. (1974) *J. Exp. Med. 140*, 1676–1695.

Luedtke, R., Owen, C. S., & Karush, F. (1980) *Biochemistry 19*, 1182–1192.

Maeyama, K., Hohmann, R. J., Metzger, H., & Beaven, M. A. (1986) *J. Biol. Chem. 261*, 2583–2592.

Margenau, H., & Murphy, G. M. (1956) *The Mathematics of Physics and Chemistry*, Van Nostrand, New York.
Mazurek, N., Schindler, H., Schurholz, Th., & Pecht, I. (1983) *Proc. Natl. Acad. Sci. U.S.A. 81*, 6841-6845.
Menon, A. K., Holowka, D., & Baird, B. (1984) *J. Cell. Biol. 98*, 577-583.
Menon, A. K., Holowka, D., Webb, W. W., & Baird, B. (1985) *J. Cell Biol. 102*, 534-540.
Menon, A. K., Holowka, D., Webb, W. W., & Baird, B. (1986a) *J. Cell Biol. 102*, 534-540.
Menon, A., Holowka, D., Webb, W. W., & Baird, B. (1986b) *J. Cell Biol. 102*, 541-550.
Pecht, I., Haselkorn, D., & Friedman, S. (1972) *FEBS Lett. 24*, 331-338.
Poljak, R. J. (1978) *CRC Crit. Rev. Biochem.* 45-84.
Rudolph, A. K., Burrows, P. D., & Wahl, M. R. (1981) *Eur. J. Immunol. 11*, 527-529.
Sagi-Eisenberg, R., & Pecht, I. (1984) *EMBO J. 3*, 497-500.
Schechter, I., & Berger, A. (1966) *Biochemistry 5*, 3362-3370.
Schlessinger, J., Webb, W. W., Elson, E. L., & Metzger, H. (1976) *Nature (London) 264*, 550-552.
Schumaker, V. N., Green, G., & Wilder, R. D. (1973) *Immunochemistry 10*, 521-528.
Schumaker, V. N., Seegan, G. W., Smith, C. A., Ma, S. K., Rodwell, J. D., & Schumaker, M. F. (1980) *Mol. Immunol. 17*, 413-423.
Schwartz, L. B., & Austen, K. F. (1984) *Prog. Allergy 34*, 271-321.
Segal, D. M., Taurog, J. D., & Metzger, H. (1977) *Proc. Natl. Acad. Sci. U.S.A. 74*, 2993-2997.
Siraganian, R. P., Hook, W. A., & Levine, B. B. (1975) *Immunochemistry 12*, 149-157.
Warner, C., & Schumaker, V. (1970) *Biochemistry 9*, 451-459.
Wilder, R. L., Green, G., & Schumaker, V. N. (1975) *Immunochemistry 12*, 35-47.

Molecular Cloning and Sequence Analysis of cDNAs Encoding Porcine Kidney D-Amino Acid Oxidase†

Kiyoshi Fukui, Fusao Watanabe, Toshihiro Shibata, and Yoshihiro Miyake*
Department of Biochemistry, National Cardiovascular Center Research Institute, Fujishiro-dai, Suita, Osaka 565, Japan
Received November 17, 1986; Revised Manuscript Received January 22, 1987

ABSTRACT: Complementary DNAs encoding D-amino acid oxidase (EC 1.4.3.3, DAO), one of the principal and characteristic enzymes of the peroxisomes of porcine kidney, have been isolated from the porcine kidney cDNA library by hybridization with synthetic oligonucleotide probes corresponding to the partial amino acid sequences. Analysis of the nucleotide sequences of two clones revealed a complete 3211-nucleotide sequence with a 5′-terminal untranslated region of 198 nucleotides, 1041 nucleotides of an open reading frame that encoded 347 amino acids, and a 3′-terminal untranslated region of 1972 nucleotides. The deduced amino acid sequence was completely identical with the reported sequence of the mature enzyme [Ronchi, S., Minchiotti, L., Galliano, M., Curti, B., Swenson, R. P., Williams, C. H. J., & Massey, V. (1982) *J. Biol. Chem. 257*, 8824-8834]. These results indicate that the primary translation product does not contain a signal peptide at its amino-terminal region for its translocation into peroxisomes. RNA blot hybridization analysis suggests that porcine kidney D-amino acid oxidase is encoded by three mRNAs that differ in size: 3.3, 2.7, and 1.5 kilobases. Comparison of the sequences of the two cDNA clones revealed that multiple polyadenylation signal sequences (ATTAAA and AACAAA) are present in the 3′-untranslated region, making the different mRNA species. The efficiency of 3′ processing of the RNA was quite different between the two signal sequences ATTAAA and AACAAA. Southern blot analysis showed the presence of a unique gene for D-amino acid oxidase in the porcine genome.

Flavoenzymes catalyze a variety of reactions by transferring one or two electrons between chemically diverse donor and acceptor molecules. D-Amino acid oxidase (EC 1.4.3.3, DAO)[1] is one of the representative flavoproteins with flavin adenine dinucleotide (FAD) as the prosthetic group that catalyzes the oxidative deamination of D-amino acids. Since the initial characterization (Krebs, 1935) and crystallization (Kubo et al., 1958; Massey et al., 1961; Yagi et al., 1962) of this enzyme, many investigations have been made to clarify the physicochemical properties and reaction mechanism of the enzyme. Systematic studies of DAO activity in various tissues revealed its existence in liver, kidney proximal tubules, certain parts of brain (Dunn & Perkoff, 1963), and granules of neutrophilic leukocytes (Cline & Lehrer, 1969). However, D-amino acids have not been found in mammalian proteins, and they do not appear to be intermediates in normal metabolism. Several lines of evidence indicating the function of the enzyme were reported (Hamilton et al., 1979; Nakajima et al., 1981), but the biological significance of this enzyme still remains to be elucidated.

Intracellular localization of DAO is reported to be in the special organelle, i.e. peroxisome (de Duve & Baukhuin, 1966), and DAO is one of the principal and characteristic enzymes of the peroxisomes of porcine kidney. This organelle has a

† This study was supported in part by a Research Grant for Cardiovascular Diseases (59C-8) from the Ministry of Health and Welfare of Japan and Grant-in-Aids for Scientific Research (61570151) and for Special Project Research (61132005) from the Ministry of Education, Science and Culture of Japan.

[1] Abbreviations: DAO, D-amino acid oxidase; bp, base pair; kb, kilobase; FAD, flavin adenine dinucleotide; PAS, periodic acid-Schiff.

0006-2960/87/0426-3612$01.50/0